Cosmological perturbations without the Boltzmann hierarchy

Marc Kamionkowski

Department of Physics and Astronomy, Johns Hopkins University, 3400 North Charles Street, Baltimore, Maryland 21218, USA

(Received 17 May 2021; accepted 12 August 2021; published 7 September 2021)

Calculations of the evolution of cosmological perturbations generally involve solution of a large number of coupled differential equations to describe the evolution of the multipole moments of the distribution of photon intensities and polarization. However, this "Boltzmann hierarchy" communicates with the rest of the system of equations for the other perturbation variables only through the photon-intensity quadrupole moment. Here I develop an alternative formulation wherein this photon-intensity quadrupole is obtained via solution of two coupled integral equations—one for the intensity quadrupole and another for the linear-polarization quadrupole—rather than the full Boltzmann hierarchy. This alternative method of calculation provides some physical insight and a cross-check for the traditional approach. I describe a simple and efficient iterative numerical solution that converges fairly quickly. I surmise that this may allow current state-of-the-art cosmological-perturbation codes to be accelerated.

DOI: 10.1103/PhysRevD.104.063512

I. INTRODUCTION

Linear-theory calculations of the evolution of primordial density perturbations provide the foundation for the interpretation of cosmic microwave background and large-scale-structure measurements. They are thus an essential tool in the construction of our current cosmological model and in the continuing quest for new cosmological physics.

The calculations, which trace back over 50 years [1], involve time evolution of a set of coupled differential equations [2] for the metric perturbations and for the dark-matter, baryon, neutrino, and photon density and velocity perturbations. There is also a (nominally infinite) "Boltzmann hierarchy" of differential equations for the higher moments (quadrupole, octupole, etc.) of the photon-intensity and photon-polarization and neutrino-momentum distributions. The photon hierarchies can be truncated at some maximum multipole moment $l_{\rm max} \simeq 30$ to provide sufficient precision for the monopole, dipole, and octupole from which the higher-order moments (which provide the CMB temperature/polarization power spectra) can be obtained through a line-of-sight integral [3]. Higher-order extensions to the tight-coupling approximation (TCA) [4,5], improved numerical integrators, and novel approximations to free-streaming relativistic particles [5]) have provided incredible code acceleration to what is still a fairly complicated numerical calculation. At present, virtually all work in cosmology now relies on two publicly available codes, CAMB [6] and CLASS [5], which combine speed and precision with model flexibility.

These codes are now extremely efficient and reliable. However, modern cosmological analyses, which employ Markov chain Monte Carlos to map the likelihood in a multidimensional parameter space, require these codes to be run repeatedly, thus employing significant computational resources. It is thus worthwhile to explore new numerical approaches. New approaches can also often provide new insights into the physics and may perhaps provide tools that can be applied to other problems.

It was realized that for primordial tensor perturbations (i.e., gravitational waves), the Boltzmann hierarchy can be replaced by a small set of integral equations (IEs) [7,8], an approach used in Refs. [9,10]. A similar approach was discussed for scalar perturbations (primordial density perturbations) in Ref. [11], but not implemented numerically.

Here, I revisit this integral-equation approach for primordial density perturbations. I discuss simplifications to the equations in Ref. [11] and describe a specific implementation where the Boltzmann hierarchy for all photon intensity/polarization multipole moments from the quadrupole ($l = 2$) and higher are replaced by two IEs, one for the photon quadrupole, and another for the polarization quadrupole. I discuss the numerical solution of these integral equations and how the initial conditions for the IEs are set from an early-time solution obtained with the TCA. I describe an iterative algorithm to solve these integral equations simultaneously with the differential equations for the other perturbation variables. I show results from two simple numerical codes that are identical except for the replacement of the photon Boltzmann hierarchy in the first with the two integral equations in the second. Numerical experiments with these codes suggest that this iterative IE algorithm may, with further work, allow current state-of-the-art codes to be accelerated.

This paper is organized as follows. Section II presents and discusses the integral equations. Section III provides the differential equations for the other perturbation variables (i.e., for neutrinos, dark matter, baryons, and the metric) and describe how the two integral equations are combined with these other equations. Section IV describes a simple algorithm to solve the integral equations numerically and how the initial conditions for the IE solver are obtained from the tight-coupling approximation at early times. This section also describes an iterative algorithm to solve them in tandem with the differential equations. Section VI describes the two rudimentary codes to evolve the Boltzmann hierarchy and the IE equations. I then present and discuss results of the calculation. Section VII concludes with a discussion of possible concerns and ideas for further steps. Appendix A provides the photon Boltzmann equations in the notation used here, and Appendix B provides details of the algorithm to solve the integral equation. The codes are provided at [12] for readers interested in following up on calculational details that cannot be inferred from the presentation here.

II. FORMALISM

If we have a spectrum of initial curvature fluctuations with power spectrum $P_{\mathcal{R}}(k) = \langle|\mathcal{R}_{\vec{k}}|^2\rangle$, then the CMB temperature/polarization power spectra are

$$C_l^{\mathrm{XX}'} = (2\pi^2)^{-1}\int k^2 dk P_{\mathcal{R}}(k)\Delta_{kl}^{\mathrm{X}}(\tau_0)\Delta_{kl}^{\mathrm{X}'}(\tau_0), \quad (1)$$

for $\mathrm{X}, \mathrm{X}^{`} = \mathrm{T}, \mathrm{E}$ with "T" the temperature and "E" the E-mode of the polarization. The transfer functions $\Delta_{kl}^{\mathrm{X}}(\tau)$ are obtained through solution of differential equations for the time evolution of the relativistic gravitational potentials, the baryon, dark-matter, photon, and neutrino densities and bulk velocities, and the higher moments of the photon and neutrino momentum distributions. The moments of the intensity distribution of photon momenta are the transfer functions $\Delta_{kl}^{\mathrm{T}}(\tau)$ and the moments of the distribution of photon polarizations are $\Delta_{kl}^{\mathrm{E}}(\tau)$.

The temperature transfer functions can be written as[1]

$$\Delta_{kl}^{\mathrm{T}}(\tau) = \int_{\tau_i}^{\tau} d\tau' g(\tau,\tau')\left\{\left[-\frac{1}{6}\frac{\dot{h}_k(\tau')}{\dot{\kappa}(\tau')} + \Delta_{k0}^{\mathrm{T}}(\tau')\right] j_l(x) - \left[\frac{1}{3}\frac{\dot{\alpha}_k(\tau')}{\dot{\kappa}(\tau')} + \frac{1}{2}\Pi_k(\tau')\right] R_l^{\mathrm{LL}}(x) + \theta_{bk}(\tau')\frac{j_l'(x)}{k}\right\}, \quad (2)$$

where $x = k(\tau - \tau')$; a dot denotes a partial derivative with respect to τ; and $g(\tau,\tau') = (d/d\tau')e^{-\kappa(\tau,\tau')} = \dot{\kappa}(\tau')e^{-\kappa(\tau,\tau')}$ is the visibility function. The initial conformal time τ_i must be taken to be deep in the tight-coupling regime and will be discussed more below. Here, $\dot{\kappa}(\tau) = d\kappa/d\tau$ is the opacity, the derivative of the Thomson-scattering optical depth with respect to conformal time, and

$$\kappa(\tau,\tau') = \int_{\tau'}^{\tau} d\tau_1 \dot{\kappa}(\tau_1). \quad (3)$$

Also, $R_l^{\mathrm{LL}}(x) = -\frac{1}{2}[j_l(x) + 3j_l''(x)]$ [13,14] in terms of spherical Bessel functions $j_l(x)$, and $\theta_{bk}(\tau)$ is the baryon velocity. It is related to the photon velocity (suppressing hereafter the subscript k for notational economy) $\theta_\gamma(\tau) = 3k\Delta_{k1}^{\mathrm{T}}(\tau)$ through

$$\dot{\theta}_b = -\mathcal{H}\theta_b + c_s^2 k^2\delta_b + \frac{\dot{\kappa}}{R}(\theta_\gamma - \theta_b), \quad (4)$$

where $\mathcal{H}(\tau) \equiv \dot{a}/a$ and $R(\tau) \equiv (3/4)\rho_b(\tau)/\rho_\gamma(\tau)$, the scale factor in units of 3/4 of that at matter-baryon equality [$\rho_b(\tau)$ and $\rho_\gamma(\tau)$ are mean baryon and photon energy densities, respectively]. The baryon sound speed c_s is increasingly important on small scales but has little effect on the larger distance/angular scales relevant for CMB fluctuations. Here, $h(\tau)$ is the standard synchronous-gauge perturbation variable, and $\alpha(\tau) = h(\tau) + 6\eta(\tau)$ in terms of the commonly used synchronous-gauge variable $\eta(\tau)$.

The function $\Pi(\tau)$ is a linear combination of the photon-intensity and polarization quadrupoles; for simplicity, I refer to it here as the polarization quadrupole. It can also be written as an IE,

$$\Pi(\tau) = \Delta_2^{\mathrm{T}}(\tau) + 9E_2(\tau), \quad (5)$$

with

$$E_l(\tau) = \int_{\tau_i}^{\tau} d\tau' g(\tau,\tau')\frac{j_l(k(\tau-\tau'))}{(k(\tau-\tau'))^2}\Pi(\tau'). \quad (6)$$

The CMB E-mode transfer function is then $\Delta_l^{\mathrm{E}}(\tau) = (3/4)\sqrt{(l+2)!/(l-2)!}E_l(\tau)$.

A derivation of Eqs. (2) and (5) will be provided in Ref. [15] using the total-angular-momentum formalism [14], but it is easily verified that they agree with Eq. (18) in Ref. [16], Eqs. (74) and (77) in Ref. [13], and with the IEs in Ref. [7]. It can also be verified, using the relation, $(2l+1)j_l'(x) = lj_{l-1}(x) - (l+1)j_{l+1}(x)$ [which $R_l^{\mathrm{LL}}(x)$ and $j_l'(x)$ also satisfy], that differentiation of these two IEs recovers the usual Boltzmann hierarchy as given, for example, in Eqs. (2.4) of Ref. [5] or Eq. (63) of Ref. [17]. Thus, these two IEs are formally equivalent to the Boltzmann hierarchy. For completeness, the Boltzmann

[1]The notation here resembles largely that in Ref. [5]. The differences are that (i) the photon Δ_{kl}^{T} here is one quarter of theirs; (ii) the R here is the inverse of their R; (iii) the $\dot{\kappa}$ here is their τ_C^{-1}; (iv) the α here is their $h + 6\eta$. The Π here is the same as that in Ref. [3] and is $\Pi = (F_{\gamma 2} + G_{\gamma 0} + G_{\gamma 2})/4$ in terms of the variables in Ref. [5].

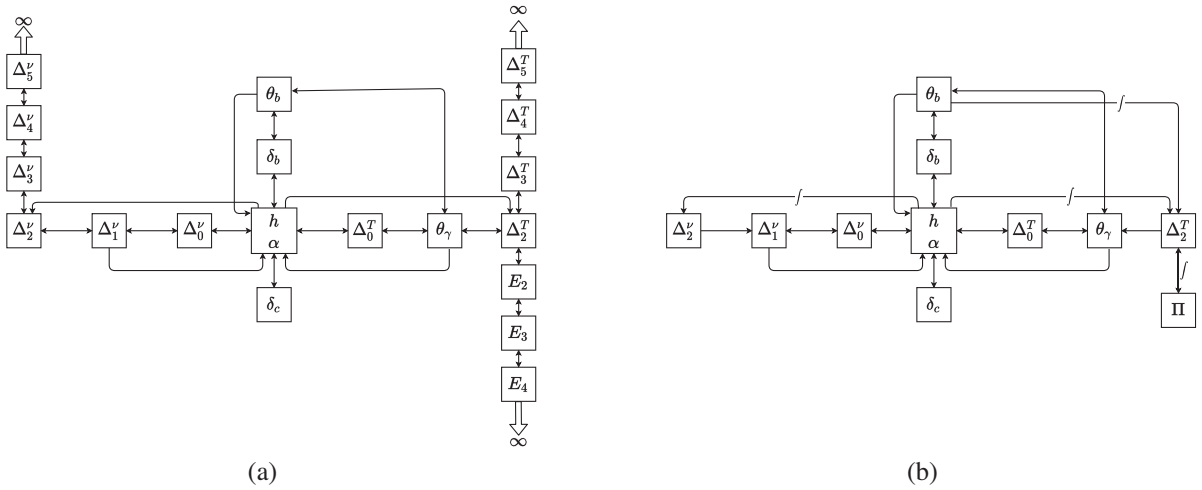

FIG. 1. Flowcharts for the perturbation calculation with (a) the Boltzmann hierarchy and (b) the integral-equation approach. An arrow points from an element that appears in the differential equation for the element it points to. Ingredients that appear in the integral equation for a given quantity are indicated in (b) with an integral sign. As both figures indicate, the higher moments ($l \geq 3$ for Δ_l^{T} and Δ_l^{ν} and ≥ 2 for E_l) communicate to the rest of the system of equations only through the quadrupole ($l = 2$). The diagrams also indicate that in both cases, the photon-intensity quadrupole Δ_2^{T} feeds into the rest of the system of equations only through the photon velocity θ_γ, and similarly for the neutrino quadrupole.

hierarchy is provided in the notation/conventions used here in Appendix A.

III. IMPLEMENTATION

The left flowchart in Fig. 1 shows the interdependency between the different perturbation variables in the differential equations for their evolution. In the middle are the metric-perturbation variables h and α. These are sourced by the baryon, dark-matter, neutrino, and photon densities and bulk velocities. Apart from the baryon-photon coupling that connects θ_γ and θ_b, the only communication between the different matter components is through the metric perturbations. The neutrino velocity is connected to the neutrino quadrupole Δ_2^{ν} which is then connected to an infinite tower of Boltzmann equations for the higher-order neutrino moments Δ_l^{ν} for $l \geq 3$. The same can be said for the photon velocity, except that there are two infinite Boltzmann hierarchies for the higher photon-intensity and photon-polarization moments. When considered in tandem, the photon monopole and dipole equations combine into a second-order differential equation that resembles that for a driven simple harmonic oscillator (discussed below); this describes oscillations of the amplitude of the photon-baryon fluid driven by changes in the metric perturbations and in the photon quadrupole.

In the line-of-sight approach [3], the Boltzmann hierarchy is solved up to a maximum multipole $l_{\mathrm{max}} \sim 30$ to obtain the photon monopole, dipole, and quadrupole, and Π to reasonable accuracy. The C_l are then obtained by evaluating the integrals in Eqs. (2) and (5).

As Fig. 1 illustrates, the two (nominally) infinite towers of photon differential equations—one for the temperature moments (Δ_l^{T} for $l \geq 3$) and polarization moments (E_l for $l \geq 2$)—communicate with the rest of the system of equations only through the photon-intensity quadrupole Δ_2^{T}. Thus, one can replace the two photon Boltzmann hierarchies with a pair of integral equations, one for Δ_2^{T} and another for Π. The rest of the system of equations is then exactly the same as in the Boltzmann approach.

In this approach we retain the two lowest-order equations, for the photon monopole ($l = 0$) and dipole ($l = 1$). These equations are

$$\dot{\Delta}_0^{\mathrm{T}} = -\frac{1}{3}\theta_\gamma - \frac{1}{6}\dot{h}, \qquad \dot{\theta}_\gamma = k^2(\Delta_0^{\mathrm{T}} - 2\Delta_2^{\mathrm{T}}) - \dot{\kappa}\Theta_{\gamma b}, \quad (7)$$

with $\Theta_{\gamma b}(\tau) \equiv \theta_\gamma(\tau) - \theta_b(\tau)$. These equations are supplemented by those,

$$\dot{\delta}_b = -\theta_b - \frac{1}{2}\dot{h}, \qquad \dot{\theta}_b = -\mathcal{H}\theta_b + c_s^2 k^2 \delta_b + \frac{\dot{\kappa}}{R}\Theta_{\gamma b}, \quad (8)$$

for the baryon density and velocity, respectively. There is also an equation, $\dot{\delta}_c = -\frac{1}{2}\dot{h}$, for the CDM-density perturbation (the CDM peculiar velocity vanishes in synchronous gauge).

The photon quadrupole $\Delta_2^{\mathrm{T}}(\tau)$ in Eq. (7) is obtained at early times by the TCA (up to second order in $\dot{\kappa}^{-1}$, as described in Refs. [4,5] for improved speed/precision). The two equations for the early-time evolution of θ_γ and θ_b can also be replaced by their TCA, with the slip $\dot{\Theta}_{\gamma b}$ evaluated (again, up to second order $\dot{\kappa}^{-1}$) [4,5].

At later times, the quadrupole is obtained from Eq. (2) with $l = 2$, along with Eq. (5) for the time evolution of $\Pi(\tau)$. With this approach, the equations in Eq. (7) combine to describe a driven oscillator damped by the photon quadrupole [18]. The photon quadrupole is provided at early times by the TCA and at later times from the integral equation.

For completeness, the Einstein equations are

$$\ddot{h} + \frac{\dot{a}}{a}\dot{h} = -8\pi G a^2[\delta\rho_{\rm tot} + 3\delta p_{\rm tot}], \tag{9}$$

$$\frac{k^2}{3}(\dot{h} - \dot{\alpha}) = 8\pi G a^2\left[\frac{4}{3}\bar{\rho}_\gamma\theta_\gamma + \frac{4}{3}\bar{\rho}_\nu\theta_\nu + \bar{\rho}_{\rm b}\theta_{\rm b}\right], \tag{10}$$

Note that the Einstein equations are written here in terms of the energy and momentum densities, but not the anisotropic stress. In this way, the photon-intensity quadrupole $\Delta_2^{\rm T}(\tau)$ communicates with the rest of the set of perturbation equations only through Eq. (7). The IEs for massless neutrinos are obtained from those for photons, but setting $\Pi = \dot{\kappa} = 0$. These IEs have come into play in the development of an effective ultrarelativistic-fluid approximation [5].

IV. NUMERICAL SOLUTION OF THE INTEGRAL EQUATIONS

The IEs here are Volterra equations of the second kind, which are typically solved as follows [19,20]. A pair of such equations has the form

$$f^\alpha(t) = \int_a^t K^{\alpha\beta}(t,s)f^\beta(s)ds + g^\alpha(t), \tag{11}$$

with $\alpha, \beta = 1, 2$ (and implied sum over repeated α, β not ij). They are solved on a mesh of N uniformly spaced time steps $t_i = a + ih$ with $i = 1, 2, \ldots, N$, with $h = (t-a)/N$. The integrals are then evaluated with the trapezoidal rule. The solution to the IEs is then $f_{\alpha,0} = g_{\alpha,0}$ and

$$\left(\delta^{\alpha\beta} - \frac{1}{2}hK_{ii}^{\alpha\beta}\right)f_i^\beta = h\left(\frac{1}{2}K_{i0}^{\alpha\beta}f_0^\beta + \sum_{j=1}^{i-1}K_{ij}^{\alpha\beta}f_j^\beta\right) + g_i^\beta. \tag{12}$$

For the pair of Volterra equations we deal with here, the 2×2 matrix on the left-hand side must be inverted at each time step [20]. The ordinary differential equations, which must be solved simultaneously, are simply stepped forward in time (i.e., Euler integration).

This algorithm works well if the kernels $K^{\alpha\beta}(t,s)$ are smooth and slowly varying. The visibility function in our integrands are smoothly varying after decoupling begins to occur, at redshifts $z \lesssim 1400$ ($\tau \gtrsim 230$ Mpc). The perturbation variables that multiply it, as well as the radial eigenfunctions, are also relatively smooth. The trapezoidal-rule integration therefore works reasonably well. However, for early conformal times ($\tau \lesssim 230$ Mpc) during tight coupling, when $\dot{\kappa} \gg \mathcal{H}$, the visibility function is very sharply peaked at $\tau' \to \tau$. The trapezoidal rule will therefore be inaccurate (unless we take a huge number of time steps).

To remedy this, and to improve the transition from tight coupling, we replace the trapezoidal rule in $\Delta\tau'$ with one in $de^{-\kappa(\tau,\tau')}$. More precisely, we write the integrand in terms of the visibility function, $(d/d\tau')e^{-\kappa(\tau,\tau')}$, times the more slowly varying perturbation variables. The integrals can then be written

$$I(\tau) = \int^\tau d\tau' f(\tau')\frac{d}{d\tau'}[e^{-\kappa(\tau,\tau')}]f(\tau)$$
$$\simeq \sum_{n=1}\int_{\kappa_n}^{\kappa_{n-1}} d(e^{-\kappa(\tau,\tau')})\left[f_{n-1} + \left(\frac{df}{d\kappa'}\right)_{n-1}(\kappa - \kappa')\right], \tag{13}$$

where $\kappa_n = \kappa(\tau - nh)$, and h is the small conformal-time step. The remaining κ' integrals can then be done analytically and the derivative $df/d\kappa'$ approximated by differencing. Details are provided in Appendix B.

By expanding the integrand $f(\tau)$ to linear order, as in Eq. (13), we obtain a result that is exact for variations of $f(\tau)$ that are up to linear in κ. At early times, this then reproduces the first-order TCA (to order $\dot{\kappa}^{-1}$), even for one step that is not necessarily small compared with $\dot{\kappa}^{-1}$. The second-order TCA is then recovered by evaluating the IE with two time steps. This allows a smooth transition from the TCA approximation to the IE algorithm in Appendix B as long as the TCA values for the perturbation variables are stored for at least two time steps. At late times, the visibility function in Eq. (13) can be Taylor expanded to linear order in $\Delta\kappa$. Doing so then recovers the trapezoidal scheme in Eq. (12).

The formula in Eq. (12) requires for each time step i a sum over all earlier time steps $j < i$. However, given the $e^{-\kappa(\tau,\tau')}$ factor in the visibility function in the integrand, the sum can for all practical purposes be started, for any given τ_i at some j such that $\kappa(\tau_i,\tau_j) \le \Delta\tau_{\rm max} \simeq 10$–$20$. If the other factors in the integrand are slowly varying, this yields a precision degradation of $\lesssim e^{-\Delta\tau_{\rm max}}$.

When the IE solver first begins, the photon-baryon fluid is still tightly coupled, and so the visibility function has support only over values of τ' fairly close to τ; i.e., $(\tau - \tau') \lesssim N\dot{\kappa}^{-1}$. The argument $x = k(\tau - \tau')$ of the radial eigenfunctions in Eq. (2) is thus small, and so the radial eigenfunctions can be approximated as $j_2(x) \simeq x^2/15$, $R_2^{\rm LL}(x) \simeq -1/5$, $j_2'(x) \simeq (2/15)x$. The integrand cannot, however, be approximated simply by the $R^{\rm LL}(x)$ term,

because Π is $\mathcal{O}(\dot{\kappa}^{-1})$ times θ_b. The third (i.e., the θ_b) term contributes, at lowest order in the TCA.

V. ITERATIVE SOLUTION OF INTEGRAL AND DIFFERENTIAL EQUATIONS

The next step is to consider how to solve the differential equations for the rest of the system simultaneously with the integral equations for the photon quadrupoles. These differential equations include those for the metric-perturbation variables, and the baryon and dark-matter densities and velocities. They also include differential equations for the neutrino perturbation variables. As the focus here is on the photon hierarchy, I will assume here that the neutrino perturbation variables can be obtained with a generalized-dark-matter [21] approximation; comments on the iterative-IE solution of the neutrino hierarchy are then presented below.

In trying to solve these differential equations in tandem with the integral equations for the photon quadrupoles, we encounter a chicken-and-egg problem: The differential equations for the rest of the system require knowledge of $\Delta_2^{\mathrm{T}}(\tau)$, but the IEs for $\Delta_2^{\mathrm{T}}(\tau)$ cannot be obtained without the solution to the DEs.

It turns out, though, that this problem can be solved with a simple iterative algorithm. Here, we start with some initial *ansatz* for $\Delta_2^{\mathrm{T}}(\tau)$ and $\Pi(\tau)$ and then solve the DEs for all the other perturbation variables with this *ansatz*. We then integrate the IEs using the solutions to those DEs to obtain new values of $\Delta_2^{\mathrm{T}}(\tau)$ and $\Pi(\tau)$. We then iterate. Of course, there is no guarantee *a priori* that this iterative procedure will converge to the correct answer, but some simple numerical experiments show that this procedure converges, and does so fairly quickly, even for a lousy [e.g., $\Delta_2^{\mathrm{T}}(\tau) = \Pi = 0$] initial *ansatz* for the IE solutions.

VI. NUMERICAL RESULTS

I have written a rudimentary C code to calculate the transfer functions for the perturbation variables with the iterative numerical implementation described here. To simplify, I approximate neutrinos (taken to be massless) as a generalized-dark-matter component with $w = c_s^2 = c_{\mathrm{vis}}^2 = 1/3$ [21]. I stop the code at redshift $z \simeq 560$, after recombination but before reionization, and use an analytic approximation (which takes into account only radiation and nonrelativistic matter at these times) for the expansion history. I use an ionization history from HyRec-2 [22]. To compare this IE approach with the standard Boltzmann hierarchy, I also wrote a second code that is identical in every way except that it swaps out the integral equations for $\Delta_2^{\mathrm{T}}(\tau)$ and $\Pi(\tau)$ for the complete photon Boltzmann hierarchy. The code uses an off-the-shelf differential-equation solver [23] with adaptive step size, although not necessarily optimized for stiff equations.

In the IE code, the handoff from the TCA to the IE solver takes place at $\tau = 160$ Mpc. The Boltzmann code uses the same TCA at early times and then starts the full Boltzmann hierarchy at $\tau = 160$ Mpc. The Boltzmann code follows the Boltzmann hierarchy up to $l_{\mathrm{max}} = 50$ (which I found was required to keep the perturbation variables stable over the τ range considered here). The results are similar, and the code a bit quicker, for smaller l_{max}. The differential-equation solver in the Boltzmann code runs with a relative error requirement of 10^{-5} and absolute error of 10^{-4}. The integral equations are evolved on a time grid that has spacing $\Delta\tau = 1.0$ from 160 Mpc $\leq \tau \leq$ 240 Mpc and 350 Mpc $\leq \tau \leq$ 450 Mpc, and $\Delta\tau = 0.5$ Mpc for 240 Mpc $\leq \tau \leq$ 350 Mpc, for a total of 401 grid points. The time required for the IE part of the calculation scales as the square of the number of grid points.

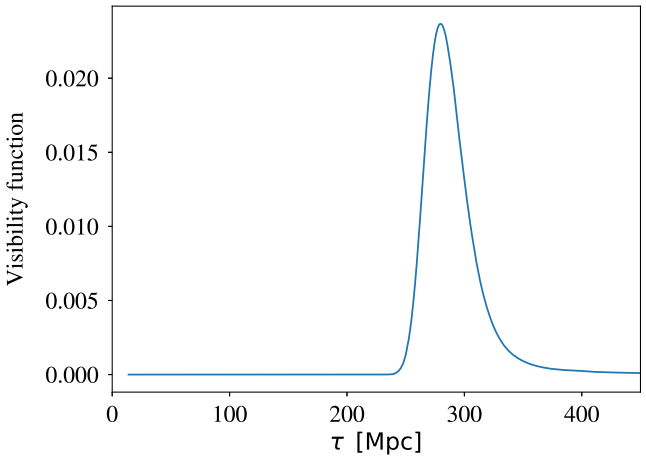

FIG. 2. The CMB visibility function $\dot{\kappa}(\tau_0, \tau)$ as a function of conformal time. It is shown to indicate the range of conformal times, peaked at $\tau \simeq 280$ Mpc, that which contribute to the observed CMB power spectra from recombination.

Figure 2 shows the visibility function, which indicates the conformal-time regime, 250 Mpc $\lesssim \tau \lesssim$ 400 Mpc, over which the source functions for the CMB power spectra are evaluated.

Figure 3 illustrates the results of the numerical experiment. Shown there are results for the photon-intensity quadrupole $\Delta_2^{\mathrm{T}}(\tau)$ of the Boltzmann code and the iterative integral-equation results, starting from a naive initial *ansatz* $\Delta_2^{\mathrm{T}}(\tau) = \Pi(\tau) = 0$. Results are shown for $k = 0.2$ Mpc, which corresponds roughly to CMB multipole moments $l \sim 3000$, near the upper limit of current measurements. The frequency of oscillations in the transfer function is reduced at smaller k, and so the numerical algorithm should, if anything, work even better at lower k.

The results are shown for one iteration (yellow), three iterations (red) and (five iterations) blue. The iterative solutions converge first at early times and then require more iterations to converge at later times. The overlap between the black and blue (five iterations) curves indicates that the agreement is at the $O(0.1\%)$ level over the conformal-time range that contributes to the observed

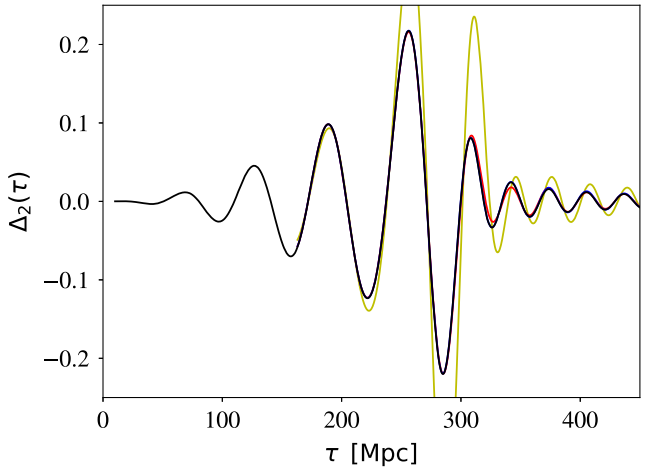

FIG. 3. The transfer function $\Delta_2^{\mathrm{T}}(\tau)$ for the CMB photon-intensity quadrupole as a function of conformal time τ for a Fourier mode of wave number $k = 0.2$ Mpc (which corresponds roughly to a CMB multipole moment $l \sim 3000$). The black curve shows the results of the full Boltzmann hierarchy as a function of conformal time. The other curves show results of the iterative integral-equation solution, taking $\Delta_2^{\mathrm{T}}(\tau) = 0 = \Pi(\tau)$ as an initial *ansatz*. The yellowish curve shows the result for $\Delta_2^{\mathrm{T}}(\tau)$ after the first iteration—i.e., after integrating the differential equations for all perturbation variables except $\Delta_2^{\mathrm{T}}(\tau)$ and $\Pi(\tau)$ and then integrating the integral equations for $\Delta_2^{\mathrm{T}}(\tau)$ and $\Pi(\tau)$ using the results of the differential equations. The red curve shows results after three iterations, and the blue curve after five iterations. The thickness of the curves is such that if two are indistinguishable, the agreement between the two is $O(0.1\%)$.

CMB power spectra. This IE code takes ∼0.15 times as long to run as the Boltzmann code, implying that each iteration can be completed in $\sim 1/30$ the time required for the Boltzmann code. Both codes are fairly rudimentary, and so these time comparisons should be taken with a grain of salt. Still, these results suggest that this may provide a route to speeding up the standard Boltzmann codes.

There may be room for even further improvement. The results shown in Fig. 3 are obtained using the most naive possible initial *ansatz* for $\Delta_2^{\mathrm{T}}(\tau)$ and $\Pi(\tau)$. The number of iterations required for convergence to the required precision can be reduced if one starts with a better initial guess for these quantities. It should be possible to derive a simple semianalytic *ansatz* that interpolates between the well-understood early-time TCA behavior and the late-time behavior, which comes from the Sachs-Wolfe effect.

One should, however, be able to do even better. These calculations are not performed in isolation. In cosmological Markov chain Monte Carlo analyses, the Boltzmann codes are run repeatedly to map the likelihood functions in a multidimensional cosmological-parameter space. Thus, each time the calculation is done, it has presumably already been done for a nearby point in that cosmological parameter space. Thus, it should be possible to start the iterative algorithm by using the results for $\Delta_2^{\mathrm{T}}(\tau)$ and $\Pi(\tau)$ from a previous run. To test this, I ran the code using as the initial *ansatz* the results for $\Delta_2^{\mathrm{T}}(\tau)$ and $\Pi(\tau)$ from a prior run with Ω_b reduced by 2%. This code converges to $O(0.1\%)$ after just one iteration.

VII. CONCLUSIONS AND IDEAS FOR FUTURE WORK

I have presented an alternative formulation of the equations for the evolution of cosmological perturbations in which the infinite Boltzmann hierarchy for the photon distribution function is replaced by a pair of integral equations. There is no new physics here—it is simply a recasting of the equations in a way that may lead to physical insight and alternative schemes for numerical solution. As was known from the line-of-sight approach [3], CMB fluctuations are determined only by the photon monopole (energy density), dipole (peculiar velocity), and quadrupole (more specifically, Π). In the Boltzmann hierarchy, these are the result of some complicated transfer of power between these lower moments of the photon distribution function and an infinite tower of higher moments. The IE formalism shows, however, that the lower moments, and in particular the quadrupole moment, at the surface of last scatter (i.e., those that enter into the line-of-sight integration) are simply described by the exact same equations that describe the lower moments that we see.

I have shown that simple iterative solution of the combined system of integral and differential equations does a pretty good job at reproducing the results of the Boltzmann calculation in a fraction of the time. This exercise also shows that the IE formalism can be implemented numerically without (apparently) any significant numerical instabilities—this was not a foregone conclusion, given the occurrence of instabilities in some IE solvers [19], as well as those that may arise from finite l_{max} in the Boltzmann hierarchy.

There is, however, far more work that needs to be done before we know whether this approach can be implemented to speed up a code like CLASS or CAMB. These codes benefit from a number of insights and clever algorithms, whereas what I have presented here is fairly naive. Those codes also have controlled errors, whereas the grid spacing in my calculation was guessed to provide an $O(0.1\%)$ precision in $\Delta_2^{\mathrm{T}}(\tau)$.

The spacing of the conformal-time grid points in the integral-equation solver is an obvious thing to explore. In this calculation I simply estimated the number of grid points that would be required for $O(0.1\%)$ precision. However, the distribution of grid points can certainly be optimized to provide the desired observables (e.g., CMB and matter power spectra) to the required precision. Good results can probably also be obtained for smaller k with fewer grid points, given the smoother integrands at lower k. The current code also sums over all prior grid points. However, given the high opacity at early times, the sum can

be restricted only to grid points that are at an optical depth $\Delta\kappa \lesssim 5$ earlier. There are also algorithms, more sophisticated than the trapezoidal-rule algorithm used here, on a numerical solution to Volterra equations (e.g., Ref. [24]) in the literature that may be worth exploring. There may be alternative implementations of the integral/differential equations that may be better suited for numerics. For example, it should be possible to eliminate the differential equations for the photon monopole and dipole and replace the integral equation for the quadrupole $\Delta_2^{\rm T}(\tau)$ with that for the monopole $\Delta_0^{\rm T}(\tau)$. Or perhaps the differential equation for $\Delta_2^{\rm T}(\tau)$ can be included and the integral equation replaced by one for $\Delta_3^{\rm T}(\tau)$. Finally, it may be worthwhile to explore whether the convergence of the iterative algorithm can be optimized with an appropriate initial ansatz for $\Delta_2^{\rm T}(\tau)$ and $\Pi(\tau)$.

While the photon hierarchies still account for a significant fraction of the computational time of modern Boltzmann codes, they are, given the powerful ordinary differential equation solvers employed now by CLASS, no longer necessarily the rate-limiting step in these codes. Thus, the order-of-magnitude speedup observed in the numerical experiments presented here will not necessarily translate to a similar speedup in those codes for basic cosmological models. Still, the codes can become far slower when the effects of massive neutrinos are included, especially for nondegenerate neutrino masses. If neutrinos are massive, their phase-space distribution depends on the magnitude of the neutrino momentum, as well as its angle. There is thus in principle an infinitude (approximated as some finite number) of neutrino Boltzmann hierarchies, one for each neutrino-momentum magnitude. An iterative IE equation approach for neutrinos, analogous to that explored here for photons, may thus prove to be quite profitable.

ACKNOWLEDGMENTS

I thank L. Ji, R. Caldwell, D. Grin, J. Bernal, and E. Kovetz for useful discussions and comments on an earlier draft and L. Ji for noting a missing k^2 in Eq. (10) in an earlier draft. This work was supported by NSF Grant No. 1818899 and the Simons Foundation.

APPENDIX A: BOLTZMANN HIERARCHY

For completeness and comparison with prior work, I provide the Boltzmann equations for the photon moments in the notation used here. These equations are derived by differentiating Eqs. (2) and (5) with respect to τ. The independent variable τ appears in the limit of integration, the visibility function, and in the radial eigenfunctions, and all of the radial eigenfunctions satisfy the spherical-Bessel-function relation, $(2l+1)j_l'(x) = l j_{l-1}(x) - (l+1) j_{l+1}(x)$. The monopole and dipole equations are already provided in Eq. (7). The equations for $l \geq 2$ are

$$\begin{aligned}\dot{\Delta}_l^{\rm T} &= -\dot{\kappa}\Delta_l^{\rm T} + \frac{kl}{2l+1}\Delta_{l-1}^{\rm T} - \frac{k(l+1)}{2l+1}\Delta_{l+1}^{\rm T} \\ &\quad + \frac{1}{5}\left(\frac{\dot{\alpha}}{3} + \frac{\dot{\kappa}\Pi}{2}\right)\delta_{l2}, \\ \dot{E}_l &= -\dot{\kappa}E_l + \frac{k(l-2)}{2l+1}E_{l-1} - \frac{k(l+3)}{2l+1}E_{l+1} + \frac{1}{15}\dot{\kappa}\Pi\delta_{l2},\end{aligned} \tag{A1}$$

with $\Pi = \Delta_l^{\rm T} + 9E_l$.

APPENDIX B: DETAILS OF THE IE SOLVER

We first define functions $I^{\rm T}(\tau,\tau')$ and $I^{\Pi}(\tau,\tau')$ by writing

$$\begin{aligned}\Delta_2^{\rm T}(\tau) &= \int^{\tau} d\tau' g(\tau,\tau') I^{\rm T}(\tau,\tau'), \\ \Pi(\tau) &= \int^{\tau} d\tau' g(\tau,\tau') I^{\Pi}(\tau,\tau').\end{aligned} \tag{B1}$$

The integrals are then discretized, taking into account the fact that $\Pi(\tau)$ appears in $I^{\rm T}(\tau,\tau')$ and $I^{\Pi}(\tau,\tau')$, in the following way. We define two sums,

$$\begin{aligned}\Delta_{2,i+1}^0 &= \sum_{j\leq i}(I_{j+1}^{\rm T}W_j^+ + I_j^{\rm T}W_j) - \frac{1}{10}\Pi_{j+1}W_i^+ \\ \Pi_{i+1}^0 &= \sum_{j\leq i}(I_{j+1}^{\Pi}W_j^+ + I_j^{\Pi}W_j) - \frac{3}{5}\Pi_{i+1}W_j^+,\end{aligned}$$

where $\Pi_i = \Pi(\tau_i)$, $I_j^{\rm T} = I^{\rm T}(\tau_{i+1},\tau_j)$, and $I_j^{\Pi} = I^{\Pi}(\tau_{i+1},\tau_j)$. Here the weight functions are

$$\begin{aligned}W_j^+ &= e^{-\kappa(\tau_{i+1},\tau_{j+1})}\left(1 - e^{-\Delta\kappa_j} - \frac{1-(1+\Delta\kappa_j)e^{-\Delta\kappa_j}}{\Delta\kappa_j}\right), \\ W_j &= \frac{e^{-\kappa(\tau_{i+1},\tau_{j+1})}}{\Delta\kappa_j}[1-(1+\Delta\kappa_j)e^{-\Delta\kappa_j}],\end{aligned} \tag{B2}$$

where $\Delta\kappa_j = \kappa(\tau_{j+1}) - \kappa(\tau_j)$. These weight functions approach $W_j^+ \to \Delta\kappa_j/2$ and $W_j \to \Delta\kappa_j/2$ at late times, thus recovering Eq. (12) (written as an integral over κ, rather than τ). At early times, $W_j^+ \to 1-(\Delta\kappa)^{-1}$ and $W^j \to (\Delta\kappa)^{-1}$; this then recovers the first-order tight-coupling approximation, $\Delta_2 = (2/5)\Pi = (4/45)(\dot{\alpha}+2\theta_b)/\dot{\kappa}$, even from one time step in the evaluation of the integral—the second-order TCA is reproduced by two time steps.

The discretized quadrupoles are then

$$\begin{aligned}\Pi_{i+1} &= \frac{\Pi_{i+1}^0 + \Delta_{2,i+1}^0}{1-\frac{7}{10}W_i^+}, \\ \Delta_{2,i+1}^{\rm T} &= \Delta_{2,i+1}^0 + \frac{1}{10}\Pi_{i+1}^0 W_i^+.\end{aligned} \tag{B3}$$

[1] R. A. Sunyaev and Y. B. Zeldovich, Small scale fluctuations of relic radiation, Astrophys. Space Sci. **7**, 3 (1970); P. J. E. Peebles and J. T. Yu, Primeval adiabatic perturbation in an expanding universe, Astrophys. J. **162**, 815 (1970); J. Silk, Fluctuations in the primordial fireball, Nature (London) **215**, 1155 (1967).

[2] J. R. Bond and G. Efstathiou, Cosmic background radiation anisotropies in universes dominated by nonbaryonic dark matter, Astrophys. J. **285**, L45 (1984); The statistics of cosmic background radiation fluctuations, Mon. Not. R. Astron. Soc. **226**, 655 (1987); M. L. Wilson and J. Silk, On the anisotropy of the cosmological background matter and radiation distribution. 1. The radiation anisotropy in a spatially flat universe, Astrophys. J. **243**, 14 (1981); N. Vittorio and J. Silk, Fine-scale anisotropy of the cosmic microwave background in a universe dominated by cold dark matter, Astrophys. J. **285**, L39 (1984).

[3] U. Seljak and M. Zaldarriaga, A line of sight integration approach to cosmic microwave background anisotropies, Astrophys. J. **469**, 437 (1996).

[4] F. Y. Cyr-Racine and K. Sigurdson, Photons and baryons before atoms: Improving the tight-coupling approximation, Phys. Rev. D **83**, 103521 (2011).

[5] D. Blas, J. Lesgourgues, and T. Tram, The cosmic linear anisotropy solving system (CLASS) II: Approximation schemes, J. Cosmol. Astropart. Phys. 07 (2011) 034.

[6] A. Lewis, A. Challinor, and A. Lasenby, Efficient computation of CMB anisotropies in closed FRW models, Astrophys. J. **538**, 473 (2000).

[7] S. Weinberg, Damping of tensor modes in cosmology, Phys. Rev. D **69**, 023503 (2004).

[8] D. Baskaran, L. P. Grishchuk, and A. G. Polnarev, Imprints of relic gravitational waves in cosmic microwave background radiation, Phys. Rev. D **74**, 083008 (2006).

[9] R. Flauger and S. Weinberg, Tensor microwave background fluctuations for large multipole order, Phys. Rev. D **75**, 123505 (2007).

[10] J. R. Pritchard and M. Kamionkowski, Cosmic microwave background fluctuations from gravitational waves: An analytic approach, Ann. Phys. (Amsterdam) **318**, 2 (2005).

[11] S. Weinberg, A no-truncation approach to cosmic microwave background anisotropies, Phys. Rev. D **74**, 063517 (2006).

[12] https://github.com/marckamion/IE.

[13] W. Hu and M. J. White, CMB anisotropies: Total angular momentum method, Phys. Rev. D **56**, 596 (1997).

[14] L. Dai, M. Kamionkowski, and D. Jeong, Total angular momentum waves for scalar, vector, and tensor fields, Phys. Rev. D **86**, 125013 (2012).

[15] L. Ji and M. Kamionkowski (to be published).

[16] M. Zaldarriaga and U. Seljak, An all sky analysis of polarization in the microwave background, Phys. Rev. D **55**, 1830 (1997).

[17] C. P. Ma and E. Bertschinger, Cosmological perturbation theory in the synchronous and conformal Newtonian gauges, Astrophys. J. **455**, 7 (1995).

[18] W. Hu and N. Sugiyama, Anisotropies in the cosmic microwave background: An analytic approach, Astrophys. J. **444**, 489 (1995).

[19] P. Linz, *Analytical and Numerical Methods for Volterra Equations* (Society for Industrial and Applied Mathematics, Philadelphia, 1985).

[20] W. H. Press, S. A. Teukolsky, W. T. Vetterling, and B. P. Flannery, *Numerical Recipes in FORTRAN: The Art of Scientific Computing* (Cambridge University Press, Cambridge, 1992).

[21] W. Hu, Structure formation with generalized dark matter, Astrophys. J. **506**, 485 (1998).

[22] Y. Ali-Haimoud and C. M. Hirata, HyRec: A fast and highly accurate primordial hydrogen and helium recombination code, Phys. Rev. D **83**, 043513 (2011); N. Lee and Y. Ali-Haïmoud, HyRec-2: A highly accurate sub-millisecond recombination code, Phys. Rev. D **102**, 083517 (2020).

[23] L. Shampine and M. Gordon, *Computer Solution of Ordinary Differential Equations: The Initial Value Problem* (Freeman, San Francisco, 1975).

[24] C. T. H. Baker, A perspective on the numerical treatment of the Volterra equations, J. Comput. Appl. Math. **125**, 217 (2000).